Plasma Chem Plasma Process (2007) 27:13–22
DOI 10.1007/s11090-006-9039-x

ORIGINAL ARTICLE

Novel Catalytic Dielectric Barrier Discharge Reactor for Gas-Phase Abatement of Isopropanol

Ch. Subrahmanyam · A. Renken · L. Kiwi-Minsker

Received: 22 March 2006 / Accepted: 5 September 2006 /

Abstract Catalytic gas-phase abatement of air containing 250 ppm of isopropanol (IPA) was carried out with a novel dielectric barrier discharge (DBD) reactor with the inner catalytic electrode made of sintered metal fibers (SMF). The optimization of the reactor performance was carried out by varying the voltage from 12.5 to 22.5 kV and the frequency in the range 200–275 Hz. The performance was significantly improved by modifying SMF with Mn and Co oxide. Under the experimental conditions used, the MnO_x/SMF showed a higher activity towards total oxidation of IPA as compared to CoO_x/SMF and SMF electrodes. The complete destruction of 250 ppm of IPA was attained with a specific input energy of ~235 J/L using the MnO_x/SMF catalytic electrode, whereas, the total oxidation was achieved at 760 J/L. The better performance of the MnO_x/SMF compared to other catalytic electrodes suggests the formation of short-lived active species on its surface by the in-situ decomposition of ozone.

Keywords Volatile organic compound abatement · Non-thermal plasma · Dielectric barrier discharge · Plasma-assisted catalysis · Sintered metal fibers

1 Introduction

Isopropanol (IPA) is one of the commonly used solvents in electronic industry for cleaning the printed circuit boards and LCD monitors [1]. The recommend exposure limit for IPA in the work place is 400 ppm; higher concentration causes health problems like irritation of eyes, drowsiness, and dizziness. Therefore, a lot of effort has been made in the development of methods for the abatement of this compound [2]. IPA from industrial effluent can be recovered by adsorption into water using wet scrubbers followed by distillation or pervaporation [3]. Thermal

---

Ch. Subrahmanyam · A. Renken · L. Kiwi-Minsker (✉)
Ecole Polytechnique Fédérale de Lausanne (LGRC-EPFL), Lausanne CH-1015, Switzerland
e-mail: lioubov.kiwi-minsker@epfl.ch

oxidation of alcohols needs a high temperature in the range 600–700 °C, whereas, thermocatalytic decomposition takes place in the temperature range 250–400 °C [4, 5]. At low concentrations (<1000 ppm) these techniques are not economically feasible since the complete combustion of diluted VOCs is not possible in the autothermal regime and needs continuous heating of big air volumes. In this context, non-thermal plasma (NTP) produced at atmospheric pressure could be a method of choice. In NTP, the electrical energy is primarily utilized for the production of energetic electrons, leaving the background gas nearly at room temperature [6–13]. In addition, NTP produces active species like radicals, excited molecules and ions. When air is used as the carrier gas, ozone is also formed due to the oxygen ionization [6–16].

The NTP technique has been already tested for the destruction of 135 ppm and 400 ppm of IPA with an input energy of 400 and 700 J/L, respectively [17, 18]. However, formation of acetone as a stable secondary product was observed. Acetone destruction by NTP was found to be difficult and took place at higher SIE (~1100 J/L), which is not energetically favorable [17–19]. Hence, the development of an efficient NTP reactor towards total oxidation of IPA at reasonable input energy remains a challenge.

The NTP technique has been used for the destruction of various VOCs with the reported selectivity to CO_2 (total oxidation) of 30–50%, whereas, the target value is 100%. Among different alternatives to improve the efficiency of NTP reaction, plasma combined with a heterogeneous catalyst seems to be a suitable choice [10, 14–16]. In practice, the catalyst can be placed either in the discharge zone (*in*-plasma catalytic reactor) or after the discharge zone (*post*-plasma catalytic reactor) [14–16, 20–25]. However, both methods have limitations mainly due to the deactivation of the catalyst by carbonaceous deposits on the surface.

Recently, we reported a novel dielectric barrier discharge (DBD) reactor configuration, where a metallic catalyst made of sintered metal fibers (SMF) serves at the same time as the inner electrode [26, 27]. Destruction of toluene as a model VOC was tested and the complete oxidation of toluene was attained using SMF modified by MnO_x [26, 27]. This study presents the destruction of 250 ppm of IPA by DBD catalytic reactor aiming on the total IPA oxidation at low input energy (SIE < 800 J/L). Influence of various parameters, like the catalyst formulation, applied voltage, frequency and the formation of ozone on the performance of plasma reactor is studied.

2 Experimental

2.1 Materials and Method

Sintered metal fiber (SMF) filters made of stainless steel (Cr 16–18; Ni 10–13; Mo 2–2.5; Fe balance) in the form of a uniform pore panel (thickness 0.29 mm, porosity of 80%) were used as the inner electrode. For the deposition of 3 wt% MnO_x and CoO_x, the SMF was first oxidized at 600 °C for 4 h, followed by impregnation with Co and Mn nitrate aqueous solutions. Drying at room temperature and calcination at 773 K in air for 5 h forms metal oxide film supported on SMF. Finally, SMF catalytic filters were subjected to an electrical hot-press treatment to shape them into cylinders with an outer diameter of 11.5 mm.

Details of the novel DBD reactor with catalytic electrode have been reported elsewhere [26]. Briefly, the dielectric discharge was generated in a cylindrical quartz tube with an inner diameter of 18.5 mm. A silver paste painted on the outer surface of the quartz tube acts as the outer electrode, whereas, a stainless steel SMF filter was used as the inner electrode. Typical discharge length was 10 cm and discharge gap 3.5 mm. The SIE in the range of 160–760 J/L was applied by varying the AC high voltage (12.5–22.5 kV) and frequency (200–275 Hz). The voltage–charge (V–Q) Lissajous method was used to determine the discharge power (W) in the DBD reactor, whereas, the SIE of the discharge was calculated using the relation

$$\text{SIE (J/L)} = \text{Power (W)/gas flow rate (L/s)}$$

IPA was introduced with a motor-driven syringe pump and was diluted by a stream of air. The air flow rate was fixed at 500 mL/min (STP) using a mass flow controller (MFC). The IPA input concentration was varied between 100 and 1000 ppm by adjusting the flow rate. Air containing IPA was fed into the plasma reactor through a Teflon tube. The IPA concentration was measured at the outlet by a gas chromatograph (Shimadzu 14 B) equipped with a FID. The formation of CO_2 and CO during IPA destruction was simultaneously measured by an infrared gas analyzer (Siemens Ultramat 21-P), and the ozone formed in the plasma reactor was measured with an UV absorption ozone monitor (API-450 NEMA). As the volume change due to chemical reaction is negligible, the selectivities to CO, CO_2 and CO_x can be expressed as:

$$S_{\mathrm{CO}}(\%) = \frac{[\mathrm{CO}]}{3 \cdot \left([\mathrm{IPA}]_0 - [\mathrm{IPA}]\right)} * 100$$

$$S_{\mathrm{CO}_2}(\%) = \frac{[\mathrm{CO}_2]}{3 \cdot \left([\mathrm{IPA}]_0 - [\mathrm{IPA}]\right)} * 100$$

$$S_{\mathrm{CO}_x}(\%) = S_{\mathrm{CO}}(\%) + S_{\mathrm{CO}_2}(\%)$$

where [CO] and $[CO_2]$ are the outlet concentrations of CO and CO_2, respectively, and $[\mathrm{IPA}]_0$ and [IPA]—the initial and final isopropanol concentrations. As partially oxidized products were not observed in the present work, S_{CO_x} also represents the mass balance of the gaseous products. In order to confirm the formation of transition metal oxides on SMF surface, the XPS analysis of the modified catalytic SMF filters was carried out using an Axis Ultra ESCA system (Kratos, Manchester) with monochromated Al–K_α radiation (1486.6 eV) and reported in our earlier publication [26].

3 Results and Discussion

3.1 Discharge Characterization

Figure 1a represents a typical V–Q Lissajous figure for 22.5 kV and 275 Hz. The area of the Lissajous figure characterizes the energy dissipated during one period of

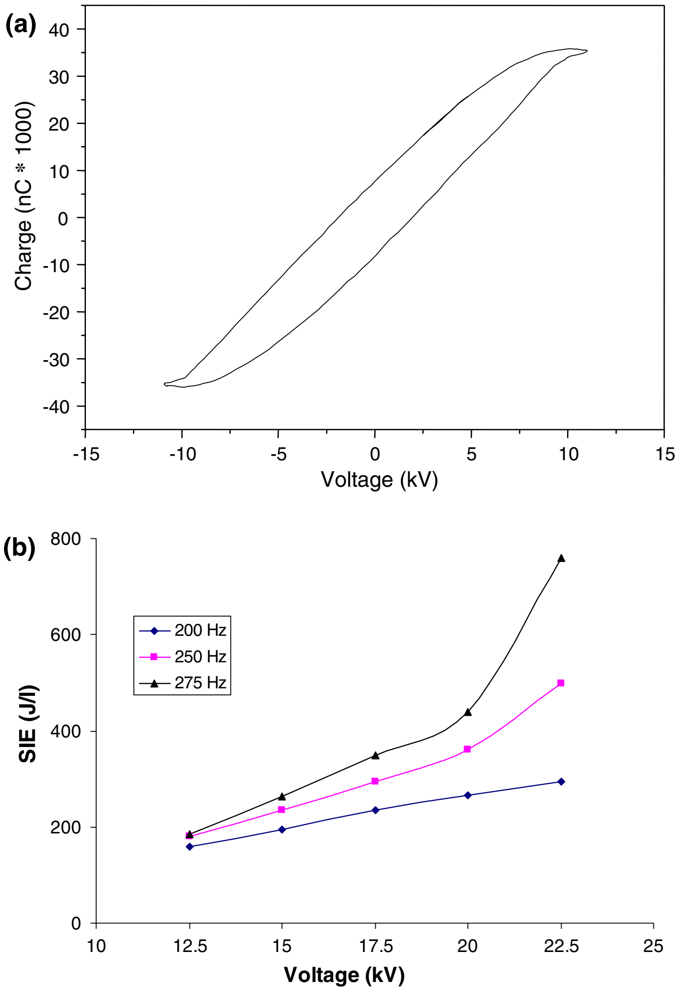

Fig. 1 (**a**) V–Q Lissajous figure of the DBD reactor for 22.5 kV and 275 Hz (**b**) Variation of SIE as a function of applied voltage and frequency

the voltage. Figure 1b represents the variation of SIE as a function of the applied voltage in the range 12.5–22.5 kV and frequency 200–275 Hz. As seen from Fig. 1b, increasing the applied voltage at a constant frequency increases the power and thereby, the SIE. For example, at 200 Hz, the SIE increased from 160 J/L (12.5 kV) to 295 J/L (22.5 kV). When the frequency was increased to 250 Hz, a considerable increase up to 500 J/L was observed. With further increasing frequency to 275 Hz, the SIE reaches a maximum value of 760 J/L at 22.5 kV.

3.2 Effect of Initial Isopropanol Concentration on the Performance of SMF Catalytic Electrodes at 195 J/L

Figure 2a shows the comparative activity of SMF electrodes as a function of IPA initial concentration varied between 100 and 1000 ppm. The experiments were

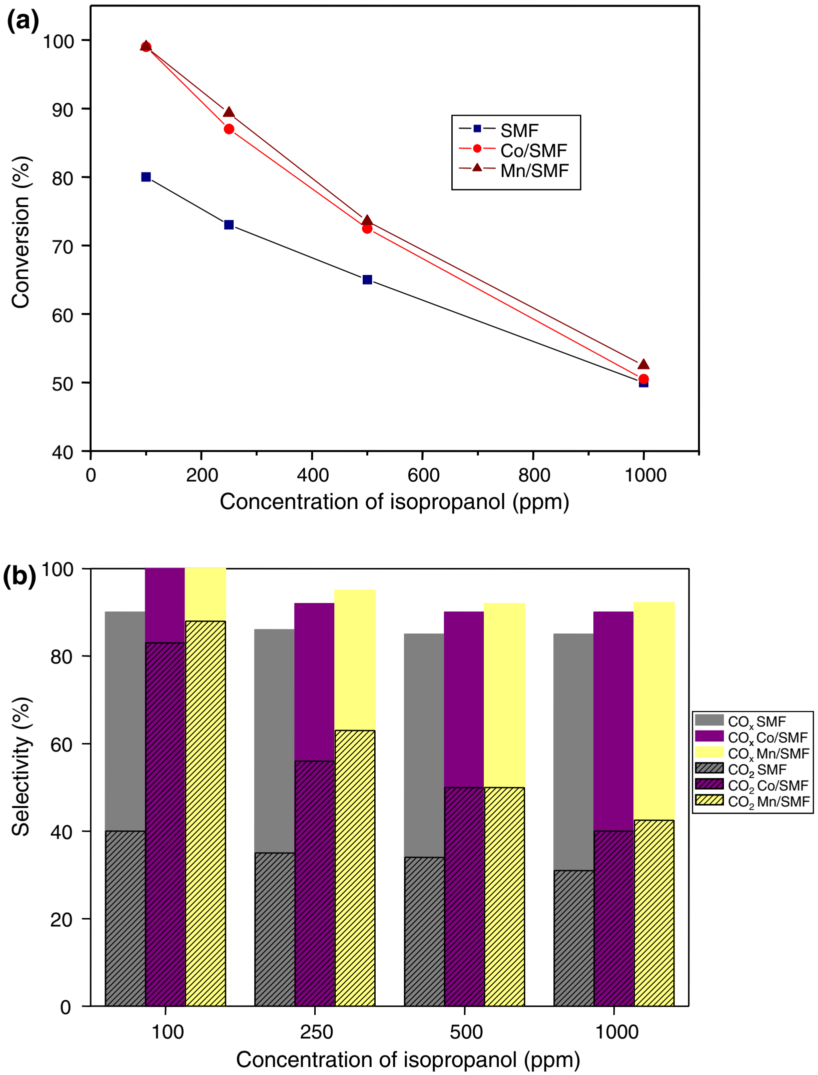

Fig. 2 Influence of initial IPA concentration at SIE of 195 J/L (15 kV and 200 Hz) on (**a**) conversion (**b**) selectivity to different products over the SMF electrodes

carried out at a voltage of 15 kV and a frequency of 200 Hz that corresponds to a SIE of 195 J/L. As seen from the Fig. 2a, the conversion decreases with increasing isopropanol concentration. For example, during the destruction of 100 ppm of isopropanol, SMF catalytic electrode showed ~80% conversion, which decreased to ~50% for 1000 ppm. A similar trend was also observed for the DBD reactor with CoO_x and MnO_x electrodes.

Figure 2b shows the selectivity to the gaseous products (CO_x, CO_2 + CO), as a function of IPA concentration (100–1000 ppm) at 195 J/L (15 kV and 200 Hz). Since partially oxidized gaseous products were not observed (CO_2 and CO are the only gaseous products formed), the solid deposited on the walls of the reactor completes the total carbon balance. Hence, as shown in Fig. 2b, for 100 ppm of IPA, at SIE 195 J/L, using SMF electrode, nearly 90% of IPA was oxidized to gaseous products, whereas, for 1000 ppm it was slightly decreased to 80% and the rest (~20%) was in the form of undesired solid deposit. Interesting observation is that at 100 ppm, metal oxide modified SMF electrodes showed ~100% selectivity to CO_x. Figure 2b also represents the selectivity to CO_2, which decreases significantly with increasing IPA concentration: for 100 ppm, the SMF electrode showed ~40% selectivity to CO_2 and dropped to ~30% for 1000 ppm. Metal oxides (Mn, Co) supported on SMF showed higher selectivity to CO_2 especially for IPA concentration <500 ppm. For example, during the destruction of 250 ppm of IPA, the MnO_x/SMF electrode showed ~60% selectivity to CO_2 against only ~30% with the SMF electrode. As explained earlier, the NTP technique would be beneficial for the abatement of diluted VOCs. Further studies were carried out at 250 ppm of IPA to optimize the performance of the SMF catalytic electrode to reach total oxidation of IPA to CO_2.

3.3 Influence of Applied Voltage on the Destruction of 250 ppm of Isopropanol over Catalytic SMF Electrodes

Conversion of 250 ppm of IPA was studied as a function of applied voltage varied in the range of 12.5–22.5 kV at a fixed frequency of 200 Hz over catalytic SMF electrodes and results were presented in Fig. 3a. These conditions correspond to the SIE of 160 and 295 J/L, respectively. As seen from Fig. 3a, the IPA conversion increases with the increasing applied voltage. However, at a particular SIE, metal oxide supported SMF electrodes showed higher conversion compared to SMF unmodified electrode. With the SMF electrode the IPA conversion reaches 100% only at 22.5 kV (295 J/L), whereas, with Co and Mn oxides supported on SMF, it was achieved at 265 J/L and 235 J/L, respectively. A similar observation was made earlier during the destruction of toluene, where MnO_x/SMF electrode showed better performance compared to CoO_x/SMF and SMF electrodes [26]. This better performance of MnO_x/SMF might be due to the formation of active oxygen species on metal oxide surface due to in-situ decomposition of ozone [6, 27].

Figure 3b represents the selectivity towards CO_x and CO_2 formed in the above experiments. As seen, during the destruction of 250 ppm of IPA, metal oxide supported SMF electrodes showed ~100% CO_x selectivity (no carbon deposit) at 17.5 kV that corresponds to a SIE 235 J/L, whereas, with the non modified SMF this was achieved only at 295 J/L (22.5 kV). Figure 3b also represents the selectivity to CO_2, which also followed the same trend as conversion and CO_x selectivity. At any voltage, MnO_x/SMF electrode showed higher CO_2 selectivity compared to CoO_x/SMF and SMF. During the present study, at 22.5 kV (295 J/L), ~75% CO_2 selectivity was achieved on MnO_x/SMF. A total conversion of 250 ppm of IPA with no carbon deposit was observed in this case (Fig. 3a, b).

3.4 Influence of Applied Voltage and Frequency on the Performance of MnO_x/SMF Catalytic Electrode during the Destruction of 250 ppm of Isopropanol

In the previous study, MnO_x catalytic electrode showed a better performance over other catalytic electrodes during the destruction of 250 ppm of IPA in the SIE range 160–295 J/L at a fixed frequency of 200 Hz. Further studies were aimed at achieving

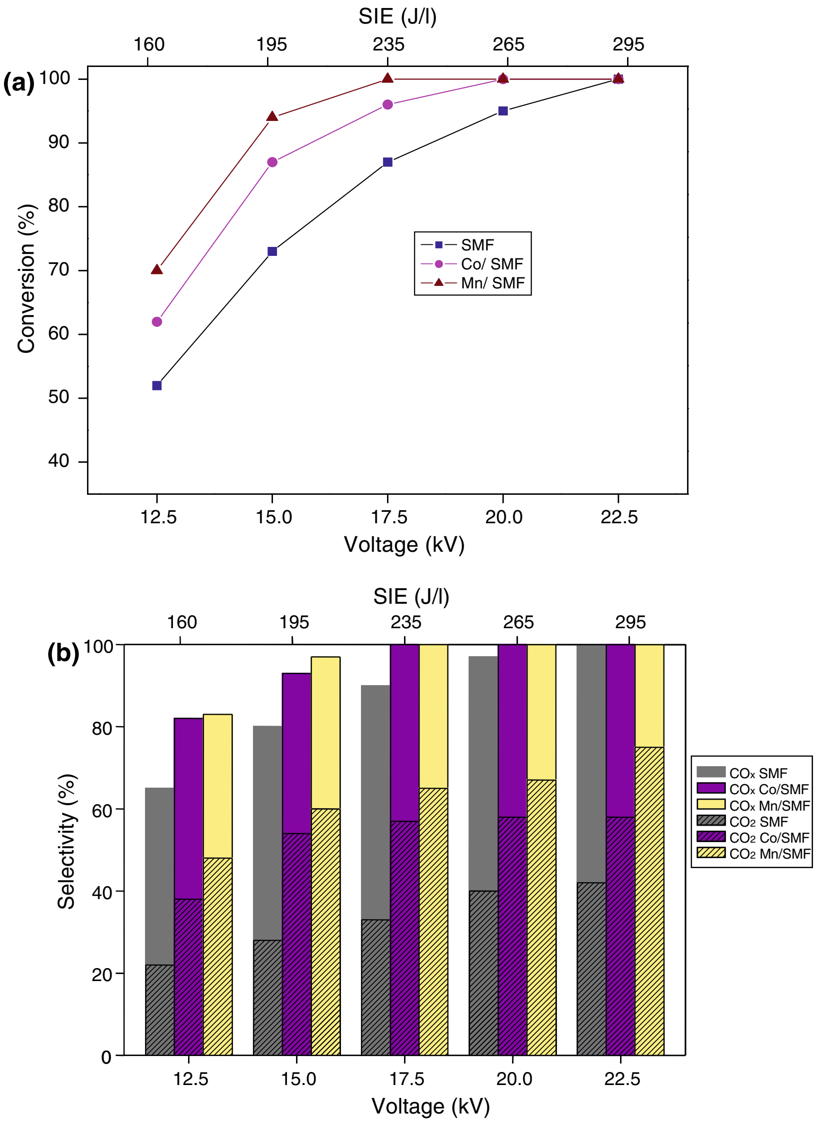

Fig. 3 Influence of voltage on (**a**) conversion (**b**) selectivity to the gas products (250 ppm of IPA, 12.5–22.5 kV, 200 Hz)

the total oxidation of 250 ppm of IPA over MnO_x catalytic electrode. Figure 4a represents relation between the SIE at different applied voltage and frequency and the efficiency of DBD reactor with MnO_x catalytic electrode. The SIE has been varied in the range 160–760 J/L by changing the applied voltage between 12.5 and 22.5 kV and frequency in the range 200–275 Hz. As seen from Fig. 4a, at 200 Hz, ~100% conversion was achieved at a SIE > 235 J/L (17.5 kV). However, with increasing frequency to 250 Hz and 275 Hz, slightly higher SIE was required to attain ~100% conversion. We assign this observation to the fact that at low voltage

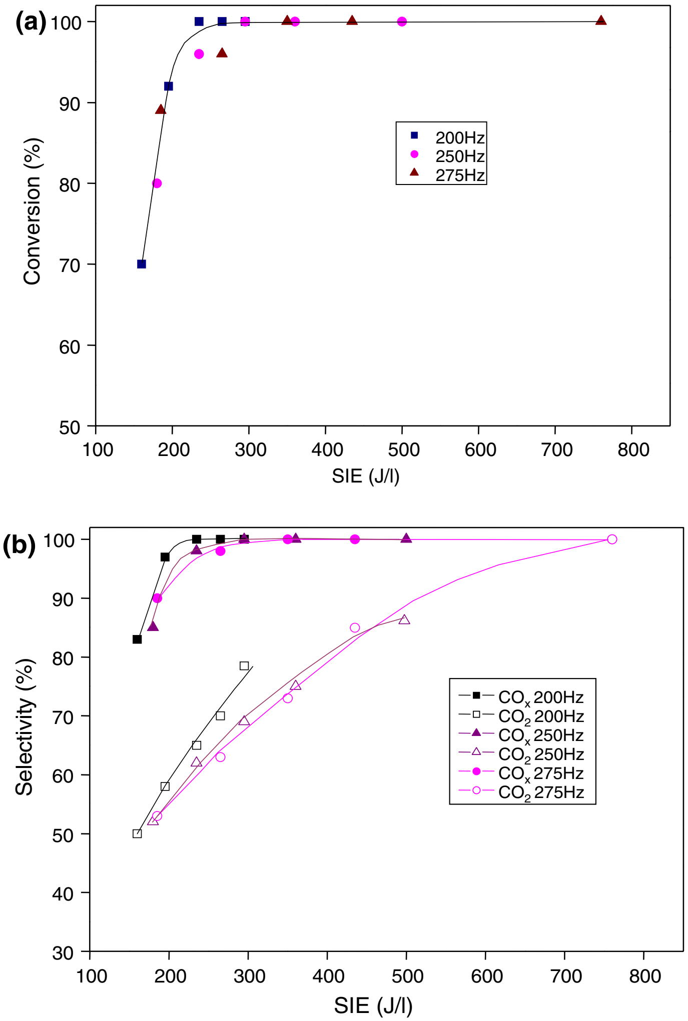

Fig. 4 Influence of SIE with the MnO_x/SMF catalytic electrode on (**a**) conversion of IPA (**b**) selectivity to the gaseous products (250 ppm of IPA, voltage 12.5–22.5 kV)

and high frequency, the conditions may be close to the ignition threshold and hence, the discharge was not uniform throughout the discharge volume. A similar observation was earlier made during the destruction of toluene in the DBD reactor [27].

Figure 4b represents the selectivity profile of the gaseous products during the destruction of IPA as a function of SIE. The selectivity of solid deposits can be estimated as (100- S_{CO_x})%. As seen from Fig. 4b, increasing both voltage and frequency lead to a higher selectivity to CO_x, but also increases SIE. At any frequency, nearly 100% selectivity to CO_x (with out solid deposit) was achieved at voltage higher 17.5 kV. Figure 4b also represents the selectivity to CO_2, which also increases with increasing SIE. When SIE was varied in the range 160–295 J/L, a maximum of 75% selectivity to CO_2 was achieved at 295 J/L (200 Hz, 22.5 kV) with ~25% selectivity to CO. Further increase of SIE to 500 J/L (22.5 kV and 250 Hz),

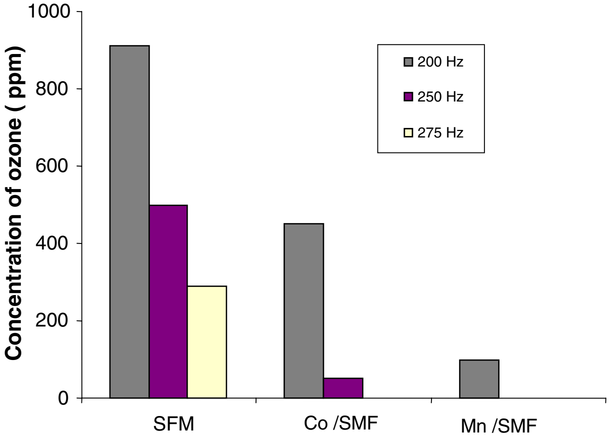

Fig. 5 Formation of ozone with the SMF catalytic electrodes (250 ppm IPA in air, 15 kV)

the CO_2 selectivity was observed to reach ~85%. Close to 100% CO_2 selectivity (no CO and carbon deposit) was achieved at 760 J/L (22.5 kV and 275 Hz). Hence, with the novel DBD reactor presented herein, it is possible to oxidize completely 250 ppm of IPA at a threshold SIE value of 760 J/L.

3.5 Ozone Formation in the DBD Reactor

It is known that NTP produces ozone from air by the ionization of oxygen molecules. There is no direct correlation between the amount of ozone formed in the NTP reactor to its efficiency, nevertheless, the oxidation of various hydrocarbons in catalytic plasma reactor might be due to the decomposition of ozone on the catalyst surface leading to the formation of strong oxidizing species, mainly atomic oxygen [6, 9, 16, 22, 23, 26, 27]. During the present study, MnO_x/SMF catalytic electrode showed better performance during the destruction of IPA compared to CoO_x/SMF and SMF. This observation can be explained based on the ozone decomposition efficiency as presented in Fig. 5, which shows the influence of the catalytic electrodes on in-situ ozone decomposition at 15 kV. With increasing frequency, the ozone concentration decreases, and the MnO_x/SMF is seen to be the most active electrode in ozone decomposition. This suggests the formation of reactive oxygen species using the MnO_x/SMF catalytic electrode at low energy consumption being responsible for the higher performance observed [6, 28, 29].

4 Conclusions

Catalytic abatement of a diluted (250 ppm) isopropanol (IPA) in air was carried out in a novel DBD reactor with a catalytic SMF electrode. The complete destruction of 250 ppm of IPA to CO_x and H_2O was achieved with a specific input energy (SIE) as low as ~235 J/L (17.5 kV and 200 Hz). Surface modification of SMF electrode with oxides of Co and Mn allowed attaining the total IPA oxidation forming only CO_2 and H_2O. Among the catalyst studied, 3wt% MnO_x/SMF showed the best performance, where a complete oxidation of IPA was achieved at SIE ~750 J/L. It has been proposed that in-situ decomposition of ozone on MnO_x/SMF leads to the formation of reactive oxygen species, which are responsible for the observed higher activity of the MnO_x/SMF catalytic electrode.

Acknowledgments The authors acknowledge the Swiss National Science Foundation (“SCOPES” program) and the Swiss Commission of Technology and Innovation (CTI, Bern) for the financial support.

References

1. http://www.cdc.gov/niosh/npg/npgd0359.html NIOSH Pocket guide to chemical Hazards, 151 2005
2. Pollution prevention and abatement handbook, World Bank Group (1998) 302
3. AWMA (1992) Air and waste management association, Air pollution engineering manual, Van Nostrand Reinhold. New York
4. Gallardo-Amores JM, Armaroli T, Ramis G, Finocchio E, Busca G (1999) Appl Catal B Environ 22:249
5. John Zink Company (1991) Innovations of catalytic combustion. International symposium on environmental control of combustion processes. Honolulu
6. Futamura S, Einaga H, Kabashima H, Hwan LY (2004) Catal Today 89:89
7. Roland U, Holzer F, Kopinke FD (2002) Catal Today 73:315
8. Futamura S, Zhang A, Prieto G, Yamamoto T (1998) IEEE Trans Ind Appl 34:967
9. Kim HH, Oh SM, Ogata A, Futamura S (2005) Appl Catal B: Environ 56:213
10. Ayrault C, Barrault J, Blin-Simiand N, Jorand F, Pasquiers S, Rousseau A, Tatibouet JM (2004) Catal Today 89:75
11. Eliasson B, Kogelschatz U (1991) IEEE Trans Ind Appl 19:1063
12. Yhang K, Eliasson B, Kogelschatz U (2002) Ind Eng Chem Res 41:1462
13. Kogelschatz U (2003) Plasma Chem Plasma Proc 23:1
14. Holzer F, Roland U, Kopinke FD (2002) Appl Catal B: Evniron 38:163
15. Roland U, Holzer F, Kopinke F.D (2005) Appl Catal B: Environ 58:217
16. Roland U, Holzer F, Kopinke FD (2005) Appl Catal B: Environ 58:227
17. Coogan JJ, Technologie Transfer # 97023244A-ENG, LANL, Feb. 1997
18. Falkenstein Z (1997) J Adv Oxid Technol 2:223
19. Oda T, Yamashita R, Takahashi T, Masuda S (1996) IEEE Trans Ind Appl 32:118
20. Tevault DE (1987) Plasma Chem Plasma Process 7:231
21. Penetratnte B, Hsiao MC, Bardsley JN, Merrit BT, Vogtlin GE, Kuthi A, Burkhart CP, Bayless JR (1997) Plasma Sources Sci Technol 6:251
22. Yamamoto T, Mizuno IK, Tamori I, Ogata A, Nifuku M, Michalska M, Prieto G (1996) IEEE Trasn Ind Appl 32:100
23. Futamura S, Zhang A, Yamamoto T (1997) J Electrostat 42:51
24. Demidiouk V, Moon SI, Chae JO (2003) Catal Commun 4:51
25. Ogata A, Mizuno K, Kushiyama S, Yamamoto T (1999) Plasma Chem Plasma Process 19:383
26. Subrahmanyam Ch, Magureanu M, Kiwi-Minsker L, Renken A (2006) Appl Catal B: Environ 65:150
27. Subrahmanyam Ch, Kiwi-Minsker L, Renken A (2006) Appl Catal B: Environ 65:157
28. Dhandapani B, Oyama ST (1997) Appl Catal B: Environ 11:129
29. Li W, Gibbs GV, Oyama ST (1998) J Am Chem Soc 120:9041